Hindawi
Geofluids
Volume 2021, Article ID 5529908, 11 pages
https://doi.org/10.1155/2021/5529908

Research Article

A Novel Model for Predicting the Well Production in High-Sulfur-Content Gas Reservoirs

Chunmei Zou,[1,2] Xiaodong Wang,[1] Jinghong Hu,[1] Yang Lv,[3] Bo Fang,[1] and Yuan Zhang[1]

[1]*Beijing Key Laboratory of Unconventional Natural Gas Geology Evaluation and Development Engineering, China University of Geosciences, Beijing, China*
[2]*Research Institute of Petroleum Exploration and Development, Beijing, China*
[3]*The Fifth Gas Production Plant in Changqing Oilfield Company, Xi'an, Shanxi, China*

Correspondence should be addressed to Jinghong Hu; hjhwhat@163.com and Bo Fang; fbcugb@foxmail.com

Received 19 February 2021; Revised 13 April 2021; Accepted 21 April 2021; Published 1 May 2021

Academic Editor: Jian-Chun Xu

High-content H_2S gas reservoirs are important for natural gas extraction. However, the precipitation and deposition of elemental sulfur in high-sulfur-content gas reservoirs eventually lead to porosity and permeability damage, resulting in the low well productivity. Therefore, it is worth developing an accurate production prediction model considering sulfur deposition for fractured horizontal wells. In this study, based on the partition model and transient percolation theory, a novel numerical model considering the damage of sulfur deposition with pressure change on reservoir porosity and permeability was first developed to predict the production from fractured horizontal wells in high-sulfur-content gas reservoirs. Then, it was validated by actual field data from a high-sulfur-content gas reservoir. After that, the influence of sulfur deposition on the production of fractured horizontal wells was revealed through theoretical calculations, and the effects of hydraulic fracture parameters on production were analyzed. The results show that elemental sulfur gradually deposits in the reservoir pores as the reservoir pressure decreases and the production time increases, which eventually leads to permeability damage and reduces reservoir productivity; this negative impact gradually increases over time. It is also shown that the production of fractured horizontal wells increases with an increase in the half-length, fracture conductivity, and fracture number. Compared with the fracture half-length, the fracture conductivity and fracture number have a greater influence on the production of a single well. The model can handle the influence of nonlinear parameters caused by sulfur deposition, which allows accurate calculations and provides guidance for the development of fractured horizontal wells in gas reservoirs with high sulfur content.

1. Introduction

During the development of high-sulfur-content gas reservoirs, elemental sulfur gradually precipitates from natural gas and deposits in reservoir pores with decreasing reservoir temperature and pressure, thus affecting gas well production [1]. Many scholars have studied the sulfur solubility model [2–5]. Fractured horizontal wells have a positive impact for delaying the pressure drop of a reservoir and alleviating sulfur deposition and precipitation; therefore, they are widely used in the development of high-sulfur gas reservoirs. According to the production data of fractured horizontal wells, there is a long-term linear flow in the production process in the log-log plot of production and time. Based on this feature, Cinco et al. [6] first proposed the concept of "bilinear flow," and Cinco and Samaniego [7] introduced this concept to the research of the production of infinite conductivity vertical fracture wells. Lee and Brockenbrough [8] developed a trilinear flow model based on bilinear flow to analyze the influence of hydraulic fracture parameters on production. Ozkan et al. [9] applied the trilinear flow model to predict the production of fractured horizontal wells in shale gas reservoirs. The results show that the trilinear flow model can meet the seepage law of shale gas flowing into fractured horizontal wells. On this basis, researchers applied the trilinear flow model to dual media and triple media conditions and divided the model into fracturing and unreformed zones considering the influence of volume fracturing [10–13].

Stalgorova and Mattar [14] proposed a five-linear flow model for hydraulic fractures and induced fractures after hydraulic fracturing and divided the reservoir into five zones from the further division of the trilinear flow model. Deng et al. [15] further considered the impact of reservoir heterogeneity on the basis of Stalgorova's model. Guo et al. [16] extended the five-linear flow model to a seven-linear flow model and divided the reservoir into seven regions. In addition to the partition model, the point source function method was applied to divide fractures into multiple nodes and then perform superposition to obtain the production performance of fractured horizontal wells [15, 17–19].

As the reservoir porosity and permeability in high-sulfur-content gas reservoirs exhibit nonlinear changes with decreases in pressure and the gas physical parameters also change, many scholars have proposed solutions to this nonlinear problem in order to simplify the mathematical equation. Agarwal [20] proposed the pseudo time method and combined the gas viscosity and compression coefficient with the time term. Kale and Mattar [21] and Kabir and Hasan [22] linearized the nonlinear term by the perturbation method based on the Boltzmann transformation. The results show that the second-order perturbation solution is sufficient for meeting engineering requirements. Ozkan et al. [9] and Apaydin [23] incorporated all nonlinear parameters by defining a new notion of pseudo pressure for nonlinear permeability changes. Eshkalak et al. [24] used the finite difference method to deal with multiple nonlinear factors and obtained good results. Hu et al. [25] developed a production model of horizontal wells in sulfur-bearing gas reservoirs based on the transient flow theory and superposition principle and described the influence of sulfur deposition on permeability, porosity, and production performance. Hu et al. [26] simplified the nonlinear term based on perturbation change and then analyzed the influence of sulfur deposition on the gas well production performance using the Douglas–Jones correction prediction, providing the dynamic characteristic curve of sulfur deposition prediction.

Although there are many studies on the production performance of fractured horizontal wells, further research on the production of fractured horizontal wells in high-sulfur-content gas reservoirs is still required. Hu et al. [26] used the stress sensitivity theory to deal with the change in porosity and permeability caused by sulfur deposition, but the sulfur solubility model is different under different temperature and pressure conditions, and the stress sensitivity model can thus be applied only for a specified reservoir. Therefore, there remain some problems in this method to address the nonlinear change of permeability. Additionally, the existing horizontal well model is mostly applied to describe conventional gas reservoirs, which cannot explain the production performance of fractured horizontal wells in sour gas reservoirs. In this study, based on the partition model and transient flow theory, the control equations of hydraulic fracture and reservoir zone are developed, and then, the control equation is solved by explicit processing of nonlinear parameters. A production prediction model for fractured horizontal wells in sour gas reservoirs is established, which can better deal with the nonlinear problems caused by sulfur deposition and avoid the complicated mathematical derivation, and the influence of sulfur deposition and engineering parameters on production is analyzed.

2. Mathematical Model of Zonal Flow in a Fractured Horizontal Well

2.1. Physical Model. In this study, the physical model of fractured horizontal well flow is shown in Figure 1. A quarter of any fracture in a fractured horizontal well is taken as the research object. According to the traditional trilinear flow hypothesis, the fluid flow zone can be divided into three parts ([9]), as shown in Figure 2: the flow in hydraulic fractures, the fracturing zone (part I), and the unreformed zone (part II). In order to fully consider the nonlinear mechanism of fluid flow in gas reservoirs with high sulfur content and address the boundary problem, the partition model needs to be further improved, and the following assumptions are made:

(1) The reservoir is homogeneous, with a uniform thickness and infinite levels, and the upper and lower boundaries are closed and saturated by elemental sulfur

(2) Constant pressure production

(3) Single-phase transient two-dimensional plane flow in the reservoir and one-dimensional flow in hydraulic fractures

(4) Natural gas physical parameters under the high pressure and the change in porosity and permeability caused by sulfur deposition are considered

2.2. Mathematical Model. Based on the above-mentioned partition model, the differential discrete mathematical simulation method is used to address nonlinear coupling problems. The finite difference model is shown in Figure 3.

For part I, the right boundary and the lower boundary are closed, and the left boundary intersects with the hydraulic fracture. For part II, the upper boundary, right boundary, and left boundary are all closed. The lower boundary of the hydraulic fracture is a constant pressure boundary.

The control equation and boundary conditions for the finite conductivity fracture are expressed as

$$\begin{cases} k_{\mathrm{f}} \dfrac{\partial^2 m}{\partial y^2} + \dfrac{2k_m}{w_{\mathrm{f}}} \dfrac{\partial m}{\partial x} = \phi c_t \dfrac{\partial m}{\partial t}, \\ \left. \dfrac{\partial m}{\partial x} \right|_{x=0, y=x_{\mathrm{f}}} = 0, \\ m|_{x=0, y=0} = m_{\mathrm{wf}}. \end{cases} \tag{1}$$

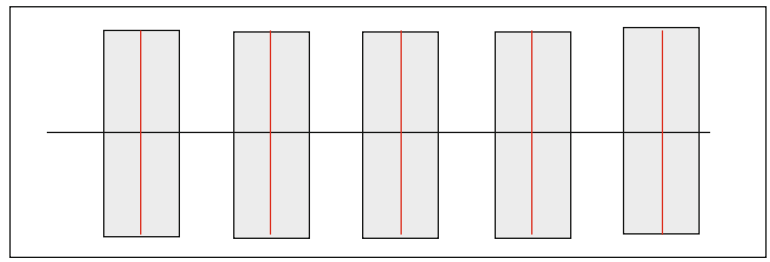

Figure 1: Physical model of the fractured horizontal well.

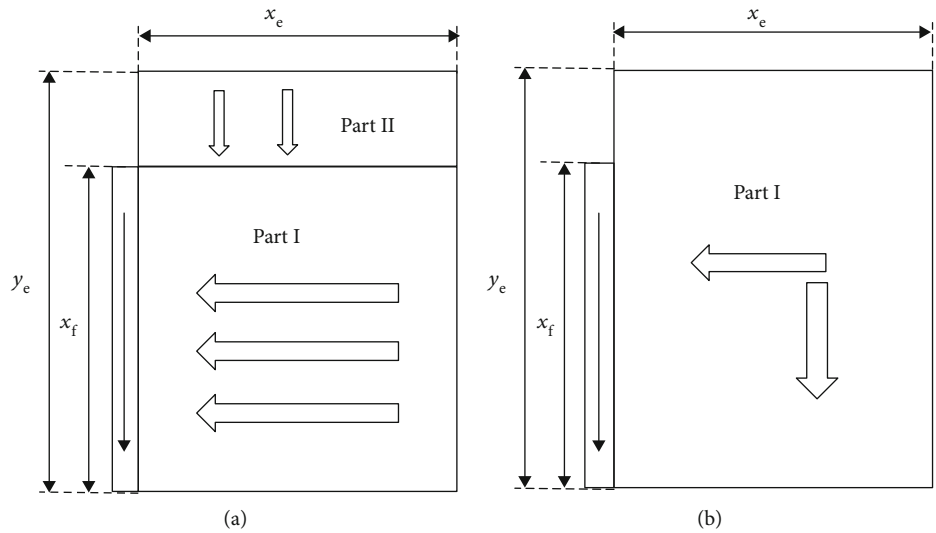

Figure 2: Partition physical model of fractured horizontal wells: (a) trilinear flow partition model and (b) partition plane flow model.

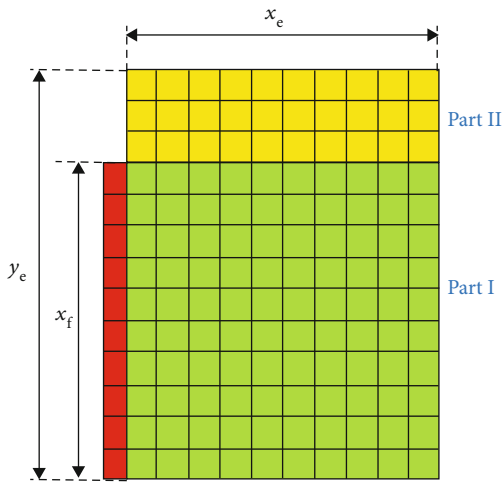

Figure 3: Diagram of the finite difference model.

The difference equation can be obtained using the numerical difference method:

$$-\frac{c_t}{\Delta t}\Delta y^2 m_{i,j}^n = \frac{4k_{1,j}\Delta y^2}{\phi_{1,j}w_f\Delta x}m_{i+1,j}^{n+1} + \frac{k_{i,j+1}}{\phi_{i,j+1}}m_{i,j+1}^{n+1} + \frac{k_{i,j-1}}{\phi_{i,j-1}}m_{i,j-1}^{n+1} - \left(\frac{4k_{1,j}\Delta y^2}{\phi_{1,j}w_f\Delta x} + \frac{k_{i,j+1}}{\phi_{i,j+1}} + \frac{k_{i,j-1}}{\phi_{i,j-1}} + \frac{c_t}{\Delta t}\right)m_{i,j}^{n+1}. \quad (2)$$

Table 1: Hu et al.' sulfur solubility model parameters [4].

Component	Natural gas density	k	a	b
$H_2S > 20\%$	<200 (kg/m^3)	1.59204	-2737.2	-8.8977
	>200 (kg/m^3)	3.2887	-4880.7	-12.497
$20\% > H_2S > 7\%$	<200 (kg/m^3)	1.38	-2582.2	-8.3938
	>200(kg/m^3)	3.2	-4880.7	-12.497
$7\% > H_2S > 6\%$	<200 (kg/m^3)	1.2	-2582.2	-8.3937
	>200(kg/m^3)	3.28	-4880.7	-12.497
$H_2S < 6\%$	<200(kg/m^3)	1.2	-2582.2	-8.3938
	>200(kg/m^3)	3.245	-4880.7	-12.497

Equation (2) can be simplified and written as

$$bm_{i+1,j}^{n+1} + dm_{i,j+1}^{n+1} + cm_{i,j-1}^{n+1} - em_{i,j}^{n+1} = -\frac{c_t}{\Delta t}\Delta y^2 m_{i,j}^n, \quad (3)$$

where $b = 4k_{1,j}\Delta y^2/\phi_{1,j}w_f\Delta x$, $d = k_{i,j+1}/\phi_{i,j+1}$, $c = k_{i,j-1}/\phi_{i,j-1}$, and $e = b + c + d + (c_t/\Delta t)y^2$. The lower boundary of the fracture is a constant pressure boundary:

$$bm_{2,1}^{n+1} + dm_{1,2}^{n+1} + cm_{wf}^{n+1} - em_{1,1}^{n+1} = -\frac{c_t}{\Delta t}\Delta y^2 m_{1,1}^n. \quad (4)$$

Table 2: Basic parameters for the model.

Parameter	Value	Parameter	Value
Reservoir porosity	0.08	Horizontal section length	600
Reservoir pressure (MPa)	39.74	Bottom pressure (MPa)	19
Reservoir permeability (m^2)	3×10^{-15}	Fracture number	5
Fracture half-length (m)	75	Fracture width (mm)	5
Reservoir thickness (m)	3.8	Fracture permeability (m^2)	30×10^{-12}
Grid number in the X direction	180	Grid length in the X direction (m)	4
Grid number in the Y direction	40	Grid length in the Y direction (m)	5

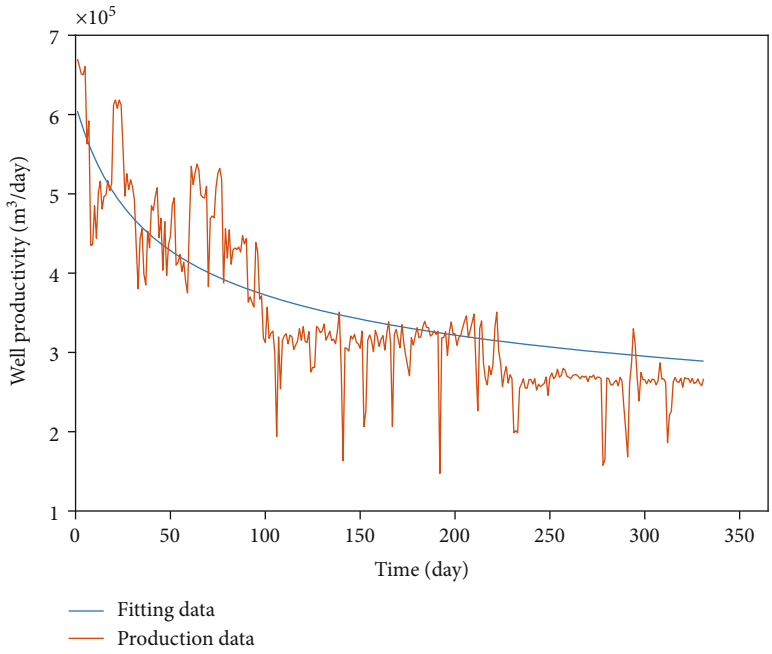

Figure 4: Comparison of the model and field production data.

In the matrix system, the governing equations and boundary conditions of fluid flow in part I and part II are

$$\begin{cases} k_x \dfrac{\partial^2 m}{\partial x^2} + k_y \dfrac{\partial^2 m}{\partial y^2} = \phi c_t \dfrac{\partial m}{\partial t}, \\ \left.\dfrac{\partial m}{\partial x}\right|_{x=0, x_f<y<y_e; y=0; y=y_e; x=x_e} = 0, \\ m|_{x=0, 0<y<x_f} = m_{wf}. \end{cases} \tag{5}$$

The difference equation can be obtained using the numerical difference method:

$$-\frac{c_t}{\Delta t}\Delta x^2 \Delta y^2 m_{i,j}^n = \frac{\Delta y^2 k_{i+1,j}}{\phi_{i+1,j}} m_{i+1,j}^{n+1} + \frac{\Delta x^2 k_{i,j+1}}{\phi_{i,j+1}} m_{i,j+1}^{n+1} + \frac{\Delta x^2 k_{i,j-1}}{\phi_{i,j-1}} m_{i,j-1}^{n+1} + \frac{\Delta y^2 k_{i-1,j}}{\phi_{i-1,j}} m_{i-1,j}^{n+1} - \left(\frac{\Delta y^2 k_{i+1,j}}{\phi_{i+1,j}} + \frac{\Delta x^2 k_{i,j+1}}{\phi_{i,j+1}} + \frac{\Delta x^2 k_{i,j-1}}{\phi_{i,j-1}} + \frac{\Delta y^2 k_{i-1,j}}{\phi_{i-1,j}} + \frac{c_t}{\Delta t}\Delta x^2 \Delta y^2\right) m_{i,j}^{n+1}. \tag{6}$$

Equation (6) can be simplified and written as

$$b m_{i+1,j}^{n+1} + a m_{i-1,j}^{n+1} + d m_{i,j+1}^{n+1} + c m_{i,j-1}^{n+1} - e m_{i,j}^{n+1} = -\frac{c_t}{\Delta t}\Delta x^2 \Delta y^2 m_{i,j}^n, \tag{7}$$

where $b = \Delta y^2 k_{i+1,j}/\phi_{i+1,j}$, $a = \Delta y^2 k_{i-1,j}/\phi_{i-1,j}$, $d = \Delta x^2 k_{i,j+1}/\phi_{i,j+1}$, $c = \Delta x^2 k_{i,j-1}/\phi_{i,j-1}$, and

$$e = a + b + c + d + \frac{c_t}{\Delta t}\Delta x^2 \Delta y^2. \tag{8}$$

For closed boundaries,

$$\begin{aligned} x = x_e &: a m_{i-1,j}^{n+1} + d m_{i,j+1}^{n+1} + c m_{i,j-1}^{n+1} - \left(a + d + c + \frac{c_t}{\Delta t}\right) m_{i,j}^{n+1} = -\frac{c_t}{\Delta t}\Delta x^2 \Delta y^2 m_{i,j}^n \frac{1}{2}, \\ x = 0, x_f < y < y_e &: b m_{i+1,j}^{n+1} + d m_{i,j+1}^{n+1} + c m_{i,j-1}^{n+1} - \left(b + d + c + \frac{c_t}{\Delta t}\right) m_{i,j}^{n+1} = -\frac{c_t}{\Delta t}\Delta x^2 \Delta y^2 m_{i,j}^n, \\ y = y_e &: b m_{i+1,j}^{n+1} + a m_{i-1,j}^{n+1} + c m_{i,j-1}^{n+1} - \left(a + b + c + \frac{c_t}{\Delta t}\right) m_{i,j}^{n+1} = -\frac{c_t}{\Delta t}\Delta x^2 \Delta y^2 m_{i,j}^n, \\ y = 0 &: b m_{i+1,j}^{n+1} + a m_{i-1,j}^{n+1} + d m_{i,j+1}^{n+1} - \left(a + b + d + \frac{c_t}{\Delta t}\right) m_{i,j}^{n+1} = -\frac{c_t}{\Delta t}\Delta x^2 \Delta y^2 m_{i,j}^n. \end{aligned} \tag{9}$$

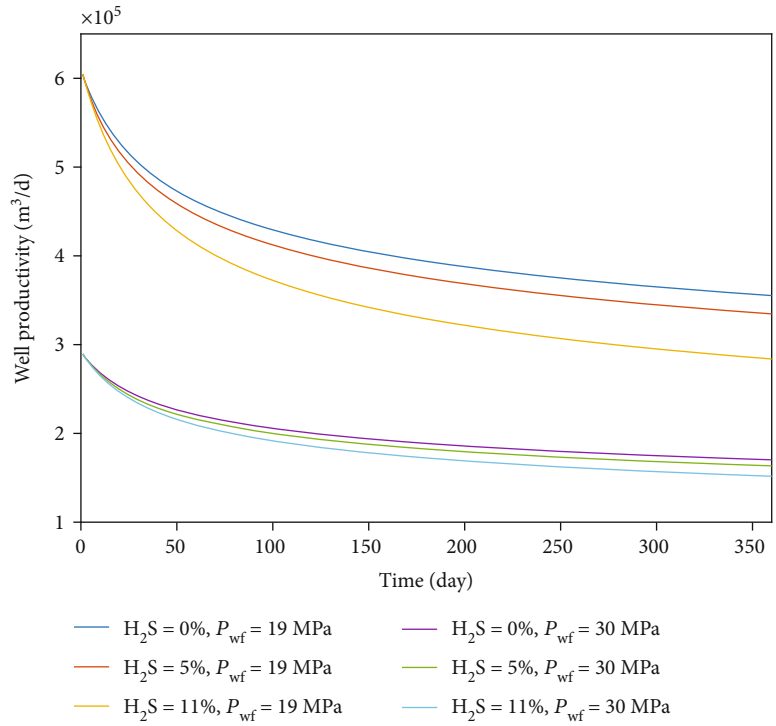

Figure 5: Effect of sulfur deposition on well productivity.

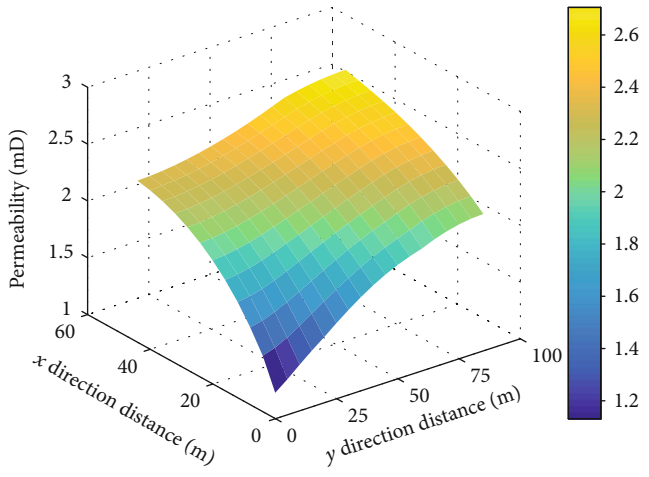

Figure 6: Reservoir permeability after 10 years of production in the 1/4 study area.

At the boundary between part I and part II, considering the continuity of fluid flow and pressure wave, both sides of the boundary can be considered to be of equal pressure and equal rate. The nonlinear parameters in the model are explicitly processed, and the pressure is implicitly processed. The coefficients of the fracture zone and matrix zone are expressed in the form of a diagonal matrix. The pressure and rate at each time step are solved by a mathematical algorithm, and then, the permeability and porosity of the grid are updated considering the influence of sulfur deposition.

The production of a single fracture is calculated by the difference between the bottom grid of the fracture and the bottom hole pressure:

$$q = w_f h k_f \frac{T_{sc}}{p_{sc} T} \frac{m_{1,1} - m_{wf}}{\Delta y}. \tag{10}$$

3. Sulfur Solubility Prediction Model

Based on the study of Chrastil [2], Roberts [3] proposed an empirical formula to predict the solubility of sulfur using a large amount of experimental data.

$$C_r = \rho^4 \left(\frac{-4666}{T - 4.5711} \right). \tag{11}$$

Hu et al. [4] analyzed the variation of sulfur solubility in natural gas with pressure and temperature:

$$C_r = \rho^k \left(\frac{a}{T + b} \right), \tag{12}$$

where the parameters k, a, and b are shown in Table 1.

With a decrease in temperature and pressure, sulfur precipitates from natural gas, and the reservoir permeability and porosity decrease due to sulfur deposition. The variation in the sulfur solubility can be expressed as

$$\Delta C = \left(\frac{\gamma}{ZT} \right)^a \exp \left(\frac{-b}{T} - c \right) (p_i^a - p^a). \tag{13}$$

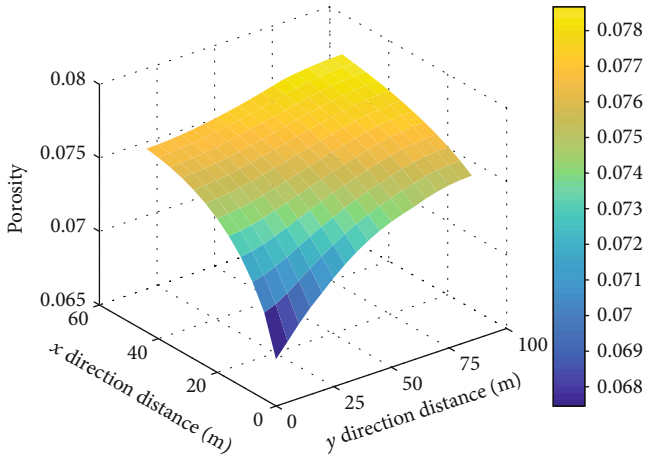

Figure 7: Reservoir porosity after 10 years of production in the 1/4 study area.

The precipitated elemental sulfur exists in the pores in the form of solid deposition, and the porosity is

$$\phi = \phi_i \left(1 - \frac{\Delta C}{\rho_s}\right). \tag{14}$$

According to Roberts [3], the relationship between permeability and porosity in gas reservoirs with high sulfur content is

$$k = k_i \exp\left[-6.22(1 - \phi/\phi_i)\right]. \tag{15}$$

By introducing equations (13) and (14) into equation (15), the change in the reservoir permeability with pressure considering the effect of sulfur deposition can be obtained by

$$k = k_i \exp\left[-6.22\left(\frac{\gamma}{ZT}\right)^a \frac{\exp\left((-b/T) - c\right)(p_i^a - p^a)}{\rho_s}\right]. \tag{16}$$

The coefficients a, b, and c in equation (16) can be selected according to different sulfur concentrations. Specific parameters can be seen in Table 1. Compared with the matrix, hydraulic fractures have a higher flow capacity, and the influence of sulfur deposition on permeability in hydraulic fractures is not considered.

If the stress sensitivity effect is taken into account, substitute it into the following equation after calculating equation (16):

$$k' = k \exp\left[-\alpha(p_i - p)\right]. \tag{17}$$

4. Results and Discussion

In order to validate the proposed model, the production data of a sulfur-bearing gas reservoir in Sichuan, China, were selected. The natural gas components are H_2S (11%), CH_4 (77%), CO_2 (8%), and N_2 (2%). The natural fractures in the reservoir do not develop, and the reservoir permeability between the hydraulic fractures does not increase significantly, so part I and part II have the same reservoir physical properties. The specific parameters used in the model are shown in Table 2, and the calculation results are displayed in Figure 4. It can be seen from the figure that the calculation results of the model in this study are roughly consistent with the actual production data, validating the proposed model.

4.1. Effects of Sulfur Deposition on Well Production. Figure 5 shows the effect of sulfur deposition on fractured horizontal well production at different H_2S concentrations and bottom hole pressure. As shown in Figure 5, the influence of sulfur deposition on production can be divided into two categories: one is the production pressure difference and the other is the concentration of H_2S. When the bottom hole pressure is 19 MPa, that is, the production pressure difference is 20 MPa; although the concentration of H_2S is only 5%, the effect of sulfur deposition on production is still obvious. And the decline gradually increases with the extension of production time. This indicates that the influence of sulfur deposition on production should be considered in the development of sulfur-bearing gas reservoirs. The effect of sulfur deposition on production was minimal when the bottom hole pressure was 30 MPa (the pressure difference was 9 MPa), and the H_2S concentration was 5%. Therefore, it can be considered that in this example, when the concentration of H_2S is less than 6% and the production pressure difference is less than 9 MPa, the effect of sulfur deposition on production can be ignored.

Figure 6 shows the reservoir permeability in the 1/4 fractured zone after ten years of production. The X direction is along the wellbore direction, and the Y direction is along the fracture propagation orientation. As displayed in Figure 6, after ten years of production, due to the decrease in reservoir pressure, sulfur components dissolved in natural gas gradually precipitate and deposit, resulting in a decrease in the reservoir permeability, and the magnitude of the decrease in permeability near the junction of the fracture and wellbore is the largest, which eventually reduces the production of fractured horizontal wells. Therefore, in the production process of fractured horizontal wells in high-sulfur-content gas reservoirs, it is necessary to control the production pressure difference to reduce sulfur deposition.

Figure 7 shows the reservoir porosity in the 1/4 fractured zone after ten years of production. As displayed in Figure 7, after ten years of production, the porosity of the reservoir gradually decreases, and the closer it is to the fracture, the porosity decreases more. This trend is also consistent with Figure 6.

4.2. Effect of Hydraulic Fracture Parameters. This proposed model is used to simulate and calculate the production change of fractured horizontal wells after one year of production. The effects of fracture half-length, fracture conductivity, and fracture number on production are analyzed as shown in Figures 8, 9, and 10, respectively.

It can be observed from Figure 8 that with a longer fracture half-length, the well productivity is higher, but the magnitude of increase in initial production gradually decreases. A larger fracture half-length leads to a larger volume of the

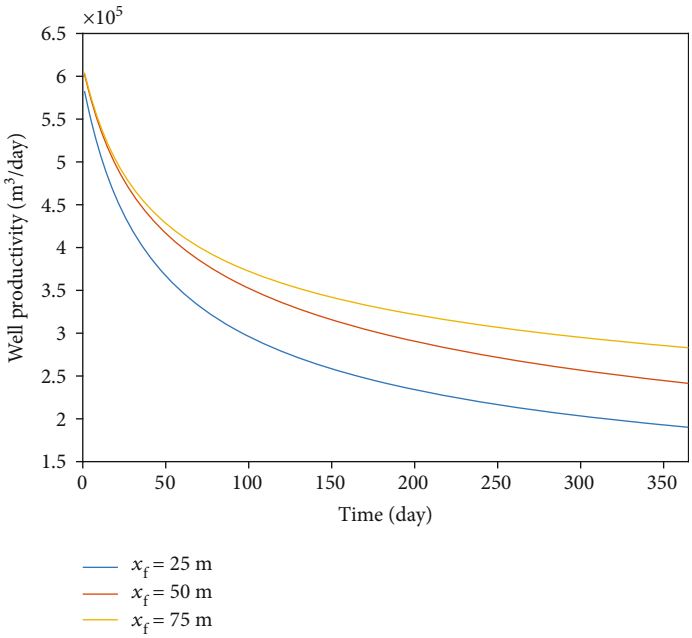

Figure 8: Effect of fracture half-length on well productivity.

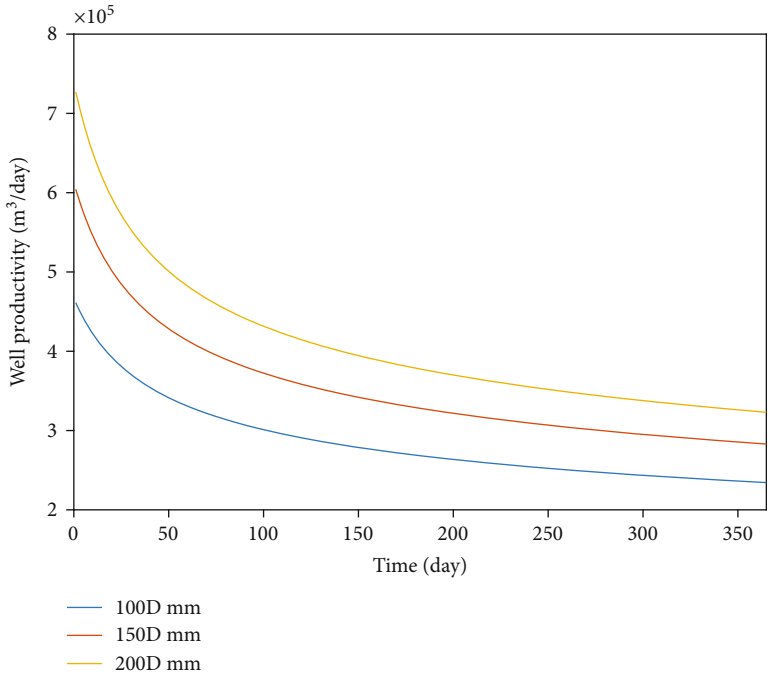

Figure 9: Effect of fracture conductivity on well productivity.

transformation area, which benefits the production of fluid from the reservoir. But the longer the fracture is, the greater the pressure loss in the fracture will be, compared with the fracture conductivity and fracture number; the influence of fracture half-length on well production is less obvious.

Figure 9 shows the influence of fracture conductivity on production. As the fracture conductivity increases, the production of fractured horizontal wells increases. Furthermore, higher production occurs not only during early production but also in the stable production period.

The fracture number has an influence on the production of fractured horizontal wells: the production increases as the fracture number increases. A greater number of fractures lead to a larger volume of the transformation zone. This implies that the fracture number is beneficial for production.

In order to study the effect of different fracture parameters on sulfur deposition, the permeability of reservoir is used to reflect sulfur deposition in this paper. Figures 11, 12, and 13 have been studied to illustrate the effects of different fracture properties on reservoir permeability. Figure 11 shows

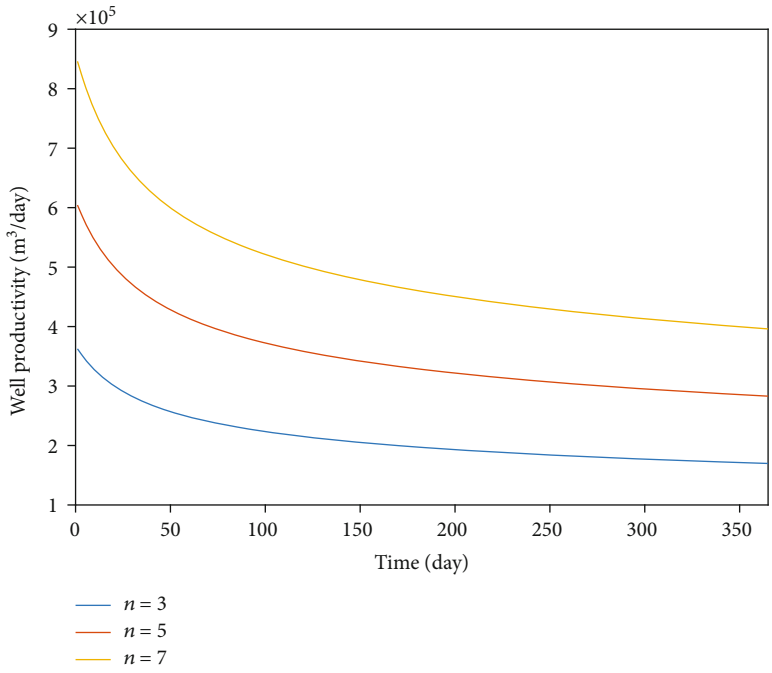

Figure 10: Effect of fracture number on well productivity.

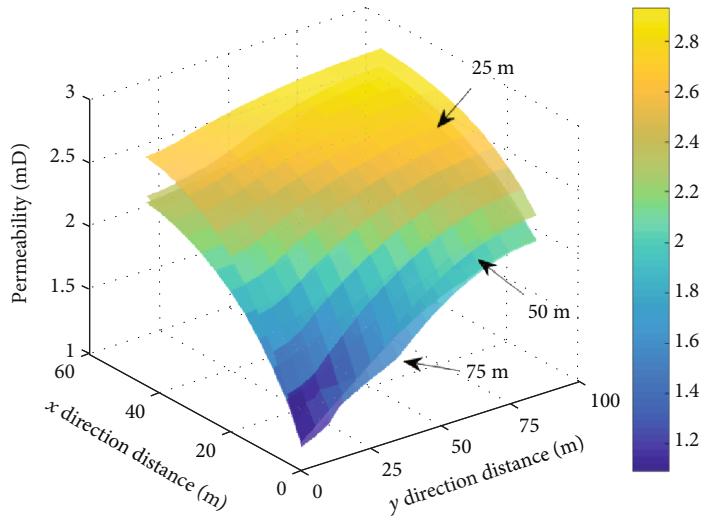

Figure 11: Effect of fracture half-length on reservoir permeability.

the effect of different fracture half-lengths on reservoir permeability. From top to bottom, layers show fracture half-lengths of 25 m, 50 m, and 75 m. It can be seen from the figure that the reservoir permeability decreases gradually as the fracture half-length increases, because the larger the fracture half-length, the higher the production. In the case of constant pressure production, this means that the production pressure difference is larger, so the sulfur deposition in the reservoir also increases correspondingly and the reservoir permeability decreases.

Figure 12 shows the effect of different fracture conductivity on reservoir permeability. From top to bottom, the layers show that the fracture conductivity is 100D mm, 150D mm, and 200D mm. As can be seen from the figure, the reservoir permeability decreases gradually with the increase in fracture conductivity, especially near the fractures, because with the increase in fracture conductivity, the greater the pressure drop near the fracture, the more the sulfur deposition.

Figure 13 shows the influence of different fracture numbers on reservoir permeability. From top to bottom, the layers show that fracture numbers are 3, 5, and 7. It can be seen from the figure that the reservoir permeability gradually decreases as the number of fractures increases. Because when the length of horizontal well remains unchanged, the more fractures there are, the smaller the spacing between fractures and the greater the pressure drop between fractures.

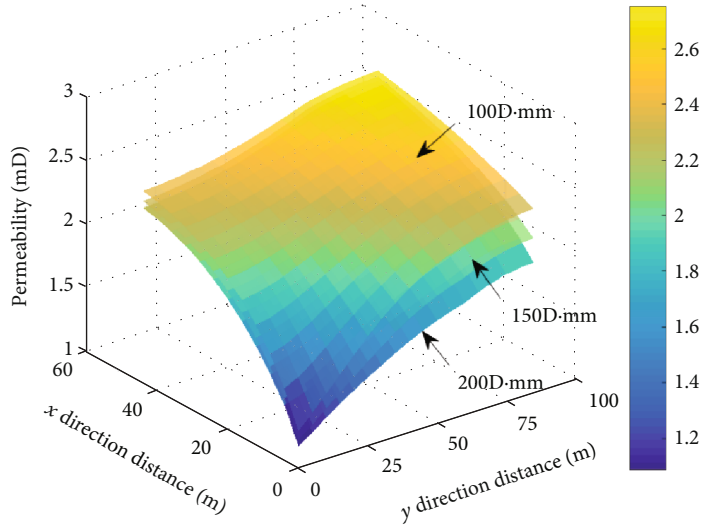

Figure 12: Effect of fracture conductivity on reservoir permeability.

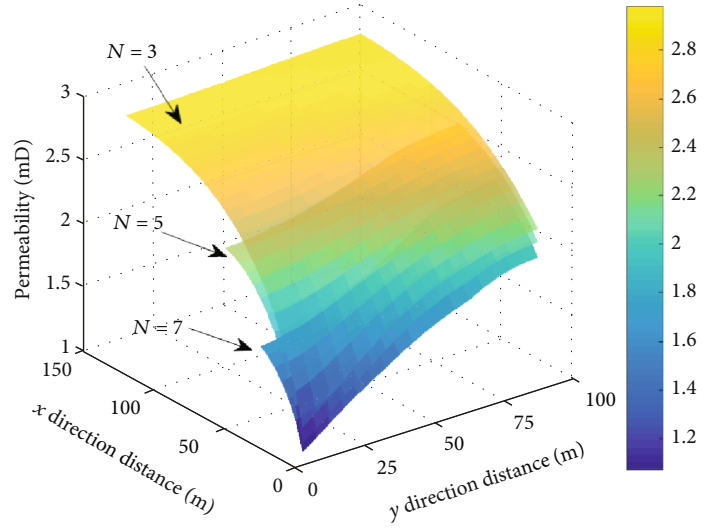

Figure 13: Effect of fracture number on reservoir permeability.

Therefore, the more obvious the difference of reservoir permeability in the X direction will be.

5. Conclusions

In this study, a novel numerical model considering the damage of sulfur deposition was developed, and the influence of sulfur deposition on the production of fractured horizontal wells was analyzed. Sensitivity analysis of different fracture parameters was conducted. The following conclusions can be drawn:

(1) Considering the nonlinear variation characteristics of permeability in high-sulfur gas reservoirs, the "implicit pressure explicit nonlinear parameter" method is used to predict the production of fractured horizontal wells in high-sulfur-content gas reservoirs. The new model can reflect the production performance and development characteristics of fractured horizontal wells in gas reservoirs with high sulfur content

(2) The accuracy of the model was verified by an example of a high-sulfur-content gas reservoir, and the influence of sulfur deposition on the production of fractured horizontal wells was revealed. As the production time increases, elemental sulfur is gradually deposited in the reservoir pores due to the decrease in reservoir pressure, resulting in a decrease in reservoir porosity and permeability, eventually leading to a decrease in production

(3) The effects of hydraulic fracture half-length, fracture conductivity, and fracture number on the production of fractured horizontal wells were analyzed. With an

increase in fracture half-length, fracture conductivity, and fracture number, the production of an individual well increases. Compared with the fracture half-length, the fracture conductivity and fracture number have a greater influence on well production

Nomenclature

C_r: Sulfur solubility (g/m^3)
C_{ri}: Initial sulfur solubility
C_t: Rock compressibility (Pa^{-1})
h: Reservoir thickness (m)
K_f: Fracture permeability (m^2)
K_m: Matrix permeability (m^2)
$m = \int(p/\mu z)dp$: Pseudo pressure
M: Molar mass (kg/mol)
P_{sc}: Standard pressure (Pa)
P_i: Initial pressure (Pa)
P_w: Wellbore pressure (Pa)
Q: Gas rate (m^3/s)
R: Universal gas constant (8.315 Pa·m^3/mol/K)
T_{sc}: Standard temperature
t: Production time (s)
W_f: Fracture width (m)
X_e: Boundary length in the X direction (m)
X_f: Fracture half-length (m)
Y_e: Boundary length in the Y direction (m)
Z: Gas compressibility factor
Φ: Matrix porosity
Φ_0: Initial matrix porosity
Δx: Space step in the X direction (m)
Δy: Space step in the Y direction (m)
Δt: Time step (s)
α: Stress effect coefficient (Pa^{-1})
ρ: Gas density (kg/m^3)
ρ_s: Solid sulfur density (kg/m^3)
μ: Gas viscosity (Pa·s)
γ: Gas-specific gravity.

Data Availability

The data used to support the findings of this study are available from the corresponding author upon request.

Conflicts of Interest

The authors declare that there is no conflict of interest regarding the publication of this paper.

Acknowledgments

The authors would like to acknowledge the support provided by the National Natural Science Foundation of China (52074248, 51804282) and Fundamental Research Funds for the Central Universities (35832019033, 35832020095).

References

[1] J. Hu, X. Yang, S. L. He, and J. Zhao, "Distribution of sulfur deposition near a wellbore in a sour gas reservoir," *Journal of Geophysics and Engineering*, vol. 10, no. 1, 2013.

[2] J. Chrastil, "Solubility of solids and liquids in supercritical gases," *Journal of Physics and Chemistry*, vol. 86, no. 15, pp. 3016–3021, 1982.

[3] B. E. Roberts, "The effect of sulfur deposition on gaswell inflow performance," *SPE Reservoir Engineering*, vol. 12, no. 2, pp. 118–123, 1997.

[4] J. H. Hu, J. Z. Zhao, L. Wang, L. Y. Meng, and Y. M. Li, "Prediction model of elemental sulfur solubility in sour gas mixtures," *Journal of Natural Gas Science and Engineering*, vol. 18, pp. 31–38, 2014.

[5] X. Guo and Q. Wang, "A new prediction model of elemental sulfur solubility in sour gas mixtures," *Journal of Natural Gas Science and Engineering*, vol. 31, pp. 98–107, 2016.

[6] L. H. Cinco, V. F. Samaniego, and A. N. Dominguez, "Transient pressure behavior for a well with a finite-conductivity vertical fracture," *SPE Journal*, vol. 18, no. 4, pp. 253–264, 1978.

[7] L. H. Cinco and V. F. Samaniego, "Transient pressure analysis for fractured wells," *Journal of Petroleum Technology*, vol. 33, no. 9, pp. 1749–1766, 1981.

[8] S. T. Lee and J. R. Brockenbrough, "A new approximate analytic solution for finite-conductivity vertical fractures," *SPE Formation Evaluation*, vol. 1, no. 1, pp. 75–88, 1986.

[9] E. Ozkan, M. Brown, R. Raghavan, and H. Kazemi, "Comparison of fractured-horizontal-well performance in tight sand and shale reservoirs," *SPE Reservoir Evaluation & Engineering*, vol. 14, no. 2, pp. 248–259, 2011.

[10] R. O. Bello and R. A. Wattenbarger, "Modelling and analysis of shale gas production with a skin effect," *Journal of Canadian Petroleum Technology*, vol. 49, no. 12, pp. 37–48, 2010.

[11] M. Brown, E. Ozkan, R. Raghavan, and H. Kazemi, "Practical solutions for pressure transient responses of fractured horizontal wells in unconventional shale reservoirs," *SPE Reservoir Evaluation & Engineering*, vol. 14, no. 6, pp. 663–676, 2011.

[12] I. G. Brohi, M. Pooladi-Darvish, and R. Aguilera, "Modeling fractured horizontal wells as dual porosity composite reservoir-application to tight gas shale gas and tight oil cases," in *SPE Western North American Region Meeting*, pp. 1–22, Anchorage, Alaska, USA, 2011.

[13] B. Xu, M. Haghighi, X. Li, and D. Cooke, "Development of new type curves for production analysis in naturally fractured shale gas/tight gas reservoirs," *Journal of Petroleum Science and Engineering*, vol. 105, pp. 107–115, 2013.

[14] K. Stalgorova and L. Mattar, "Analytical model for unconventional multi-fractured composite systems," *SPE Reservoir Evaluation & Engineering*, vol. 16, no. 3, pp. 246–256, 2013.

[15] Q. Deng, R.-S. Nie, Y.-L. Jia, X.-Y. Huang, J.-M. Li, and H.-K. Li, "A new analytical model for non-uniformly distributed multi-fractured system in shale gas reservoirs," *Journal of Natural Gas Science and Engineering*, vol. 27, pp. 719–737, 2015.

[16] J. Guo, J. Zeng, X. Wang, and F. Zeng, "Analytical model for multifractured horizontal wells in heterogeneous shale reservoirs," in *Society of Petroleum Engineers, Paper SPE-182422-MS Presented at the SPE Asia Pacific Oil & Gas Conference and Exhibition*, pp. 1–41, Perth, Australia, October 2016.

[17] Z. Chen, X. Liao, X. Zhao, X. Dou, and L. Zhu, "Performance of horizontal wells with fracture networks in shale gas formation," *Journal of Petroleum Science and Engineering*, vol. 133, pp. 646–664, 2015.

[18] W. Luo, C. Tang, and Y. Zhou, "A new fracture-unit model and its application to aZ-fold fracture," *SPE Journal*, vol. 24, no. 1, pp. 319–333, 2019.

[19] K. H. Nguyen, M. Zhang, and L. F. Ayala, "Transient pressure behavior for unconventional gas wells with finite-conductivity fractures," *Fuel*, vol. 266, 2020.

[20] R. G. Agarwal, ""Real gas pseudo-time"-a new function for pressure buildup analysis of MHF gas wells," in *SPE Annual Technical Conference and Exhibition*, pp. 1–12, Las Vegas, Nevada, USA, 1979.

[21] D. Kale and L. Mattar, "Solution of a non-linear gas flow equation by the perturbation technique," *Journal of Canadian Petroleum Technology*, vol. 19, no. 4, 1980.

[22] C. S. Kabir and A. R. Hasan, "Prefracture testing in tight gas reservoirs (includes associated papers 15913, 15964, 15989, 16469 and 16579)," *SPE Formation Evaluation*, vol. 1, no. 2, pp. 128–138, 1986.

[23] O. Apaydin, *New coupling considerations between matrix and multiscale natural fractures in unconventional resource reservoirs, [Ph.D. thesis]*, Colorado School of Mines, Golden, Colorado, 2012.

[24] M. O. Eshkalak, U. Aybar, and K. Sepehrnoori, "An integrated reservoir model for unconventional resources, coupling pressure dependent phenomena," in *SPE Eastern Regional Meeting*, pp. 1–15, Charleston, WV, USA, 2014.

[25] J. Hu, Z. Lei, Z. Chen, and Z. Ma, "Effect of sulphur deposition on well performance in a sour gas reservoir," *The Canadian Journal of Chemical Engineering*, vol. 96, no. 4, pp. 886–894, 2018.

[26] J. Hu, Z. Chen, P. Liu, and H. Liu, "A comprehensive model for dynamic characteristic curves considering sulfur deposition in sour carbonate fractured gas reservoirs," *Journal of Petroleum Science and Engineering*, vol. 170, pp. 643–654, 2018.